Kinetic Study on Catalytic Conversion of Glycerol to Renewable Acrolein

Amin Talebian-Kiakalaieh, Nor Aishah Saidina Amin*

Chemical Reaction Engineering Group (CREG), Faculty of Chemcial and Energy Engineering, Universiti Teknologi Malaysia (UTM), Johor, Malaysia, 81310.
noraishah@cheme.utm.my

Biodiesel is a suitable alternative to gasoline and diesel since it emits less carbon emission. There has been a surplus of glycerol in the market due to biodiesel production. Glycerol may be a good source of bio-based feed since it is from a renewable source. The kinetic study of gas-phase glycerol dehydration reaction using a supported γ-Al_2O_3 nanoparticle based solid heteropoly acid catalyst (SiW_{20}-Al/Zr_{10}) has been investigated. A kinetic model was established, based on the reaction mechanism, taking into account two parallel reactions of glycerol degradation into acrolein or acetol. All the reaction rate constants and activation energies were determined at various reaction temperatures (280 – 340 ˚C). The first-order kinetic model and the experimental data fitted-well. Results revealed that all the rate constants increased with temperature, and the activation energies of glycerol dehydration to acrolein and acetol were 46.0 and 53.3 kJ/mol. The results from this study are useful for simulation and process modelling of a bio-refinery for sustainable production of bio-based chemicals.

1. Introduction

Glycerol is known as a byproduct from biodiesel synthesis process. There is a surplus of glycerol supply due to increasing biodiesel production rate in the last decade (Galy et al., 2016). The utilization of biodiesel as an alternative energy source is crucial for sustainable development. Catalytic conversion of glycerol to other value-added chemicals has attracted much attention recently. Consequently, large numbers of studies have focused on the design and development of effective heterogeneous catalyst for dehydration of glycerol to acrolein (Liu et al., 2016). Acrolein is one of the most important intermediates for production of acrylic acid, methionine, 1, 3-propanediol and lactic acid. The highest ever reported acrolein selectivity was obtained by application of supported heteropoly acid catalyst in gas phase (Alhanash et al., 2010). More recently, SiW_{20}-Al/Zr_{10} catalyst registered 87.6 % acrolein selectivity at 97.1 % glycerol conversion. The catalyst exhibited long-life stability with >75 % acrolein selectivity and >80 % glycerol conversion even after 40 h reaction time, which makes it a suitable catalyst for further investigations on kinetic, mass transfer, modeling and simulation studies. Various characterization studies confirmed that catalyst activity is dominantly affected by the acidity and textural characteristics of the prepared catalyst. Also, catalyst deactivation due to coke deposition on catalyst surface is reported as the main obstacle for successful industrial application of majority of the synthesized samples (Atia et al., 2008).

There have been limited studies on the kinetics of gas phase dehydration of glycerol to acrolein. One such study was reported for a continuous system at atmospheric pressure (Park et al., 2015). Almost all the previous kinetic studies in this field were performed in supercritical water (SCW) conditions without catalyst or in presence of some simple catalyst (Qadariyah et al., 2011). Unfortunately SCW process has limited potential for industrialization due to the high production costs and inherent technical challenges (e.g. high pressure and temperature). Indeed, kinetic modeling is vital in unraveling a reaction mechanism, analyzing the catalyst characteristics effects on reaction rate, and even designing a catalyst with long-life stability and high activity. Therefore, the main objective of this paper is to conduct a comprehensive kinetic study to determine the

kinetic parameters (e.g. reaction rate constants, activation energies, and frequency factors) for all the products in glycerol dehydration reaction using a new synthesized SiW_{20}-Al/Zr_{10} solid acid catalyst.

2. Experimental

2.1 Catalyst preparation

First, catalyst with 20 wt % HSiW loading on γ-Al_2O_3 nanoparticles was prepared via the incipient-wetness impregnation method. Aqueous HSiW solution was added drop-wise to the γ-Al_2O_3 support initially. The suspension was rigorously stirred for 12 h followed by drying at 110 °C for 18 h. The HSiW-Al_2O_3 supported catalyst was denoted as SiW_{20}-Al. The final catalyst was prepared via the impregnation of 10 wt % ZrO_2 on the dried SiW_{20}-Al precursor in a similar procedure. Finally, the sample was dried at 120 °C for 18 h and referred to as SiW_{20}-Al/Zr_{10}.

2.2 Catalyst characterization

The SiW_{20}-Al/Zr_{10} catalyst was characterized by temperature-programmed desorption, elemental analyzer and the pore size and surface area were determined by Nitrogen adsorption−desorption and Brunauer, Emmett, and Teller (BET) methods, respectively. Table 1 summarizes some of the physico-chemical properties of SiW_{20}-Al/Zr_{10} for the fresh and spent catalysts.

Table 1: Physicochemical properties of catalyst

Catalyst	S_{BET} (m^2/g)	V_P (cm^3/g)	D_P (nm)	Total acidity (mmol/g.cat)	Coke (wt %)	Loading (wt %) HSiW	γ-Al_2O_3	ZrO_2
Fresh SiW_{20}-Al/Zr_{10}	96.9	0.4	19.1	2.6	-	20	70	10
Spent SiW_{20}-Al/Zr_{10}	93.0	0.4	18.2	-	1.3	20	70	10

2.3 Catalytic reaction

The gas-phase dehydration of glycerol was conducted at atmospheric pressure in a vertical packed-bed quartz reactor (30 cm length, 11 mm i.d.) using a 0.5 g catalyst sandwiched between plugs of glass wool. Prior to reaction, the catalyst was pre-treated at reaction temperature (300 °C) under nitrogen (N_2) flow (1200 mL/h) for 1 h. Liquid aqueous glycerol (10 wt %) was fed by a syringe pump at a 2 mL/h flow rate. The liquid was then vaporized in a pre-heater, mixed with inert carrier gas, and run to the reactor. The reaction products and unconverted glycerol were condensed in a water-ice-salt bath (-5 °C) and collected for analysis after 3 h of reaction. The final solution was analyzed by a gas chromatography (GC) instrument equipped with capillary column and flame ionization detector (FID). To achieve effective product separation, the column was held at 40 °C for 4 min before the temperature was ramped up to 200 °C at a rate of 12 K/min for 23 min. The glycerol conversion, acrolein selectivity, and yield are defined in Eqs (1-3).

$$Conversion_{Gl}(\%) = \frac{M_{Gl,\ in\ feed} - M_{Gl,\ in\ outlet}}{M_{Gl,\ in\ feed}} \times 100\% \tag{1}$$

$$Selectivity_N(\%) = \frac{M_{C\ in\ product}}{M_{C\ in\ Gl,\ feed} - M_{C\ in\ Gl,\ outlet}} \times 100\% \tag{2}$$

$$Yield_N(\%) = Conversion_{Gl}(\%) \times Selectivity_N(\%) \tag{3}$$

where M_{Gl} is moles of glycerol in feed or outlet streams, M_C, is moles of acrolein, and N is moles of each product. The experiments were repeated at least three times, and the average results are reported.

3. Results and discussion

3.1 Reaction route

Glycerol dehydration to acrolein has been widely studied at various (ambient and even supercritical) conditions in gas or liquid phases. Consequently, various products were reported based on application of different catalysts and reaction conditions. The major products are 3-hydroxepropanal (3-HPA), acetol, acrolein, acetaldehyde, 1,2-propanediol, acetone, acetic acid, allyl alcohol, and propanal (Tsukuda et al., 2007). Identification of the intermediate steps and by-products formation is necessary since the mechanisms, reaction rates, and activation energies related to the majority of glycerol dehydration reaction by-products are

still unknown. All the products were analysed and detected by GC and calculated based on Eqs (2-3) at different experimental conditions. Next, l logical reaction for each step is proposed based on the literature and final reaction mechanism is postulated. Figure1 illustrates a reaction mechanism proposed for glycerol dehydration to acrolein and other products using supported solid acid (SiW_{20}-Al/Zr_{10}) catalyst. The proposed mechanism reveals that acrolein is obtained after two consecutive glycerol dehydration steps. 3-HPA and acetol, products of the first dehydration step, are produced by two distinct and independent pathways. The 3-HPA is sufficiently reactive and readily converted into acrolein by the second dehydration step (R1). In fact, 3-HPA is one of the intermediate products not detected in this study due to its high reactivity compared to acrolein. However, the hydrogenation of acrolein is able to form propanal and allyl alcohol. The experimental results confers a wide range of products, including formaldehyde, 1,3-dioxan-5-ol, but the concentration of each compound was minute (R4). Acetaldehyde is formed from acrolein through the intermediate product (R3). Acetol is highly reactive and it is hydrogenated to acetone with acid catalyst (R5). Hydrogen, which is involved in the hydrogenation process, originated from the acid catalyst, Lewis acidic sites of catalyst, and coke species (Talebian-Kiakalaieh and Amin, 2015).
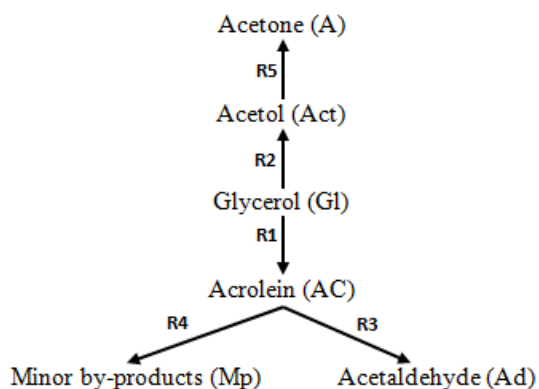

Figure 1.Simplified reaction routes for calculation of kinetic parameters

3.2 Kinetic modeling

Thus, based on results of the LHHW model in previous studies (Park et al., 2015) we can assume first order reaction for all the products. The dehydration steps (R1 and R2) are assumed to be pseudo-first order reaction (Park et al., 2015). The water molecules release during the dehydration steps (R1 and R2). However, we assumed that total amount of water is constant due to the large proportion of water (90 wt %) and little amount of glycerol (10 wt %) in the feed solution. Thus, the reaction rates of R_i can be described as Eq (4).

$$r_i = k_i . C_r \ (i = 1-5) \tag{4}$$

where, k_i is pseudo-first order kinetic rate constant, i is the number of reaction and Cr is the concentration of chemicals. Consequently, based on various reaction rates, the following differential Eqs (5-10) are obtained:

$$\frac{dC_{Gl}}{d\tau} = -k_1 C_{Gl} - k_2 C_{Gl} = -k_G C_{Gl} \tag{5}$$

$$\frac{dC_{AC}}{d\tau} = k_1 C_{Gl} - k_3 C_{AC} - k_4 C_{AC} = k_1 C_{Gl} - k_A C_{AC} \tag{6}$$

$$\frac{dC_{Act}}{d\tau} = k_2 C_{Gl} - k_5 C_{Act} \tag{7}$$

$$\frac{dC_{Ad}}{d\tau} = k_3 C_{AC} \tag{8}$$

$$\frac{dC_{Mp}}{d\tau} = k_4 C_{AC} \tag{9}$$

$$\frac{dC_A}{d\tau} = k_5 C_{Act} \tag{10}$$

where, $k_G = k_1 + k_2$ and $k_A = k_3 + k_4$.

The above ordinary differential equations (ODEs) are functions of the contact time (τ) where

$$\tau = W / F \qquad \left[\frac{Catalyst \quad weight}{Feed \quad flowrate}\right] = \left[\frac{kg - cat. \quad S}{m^3}\right] \tag{11}$$

The analytical expressions for concentrations are expressed in Eqs (12-17):

$$C_{Gl} = C_{G0}.\exp(-k_G.\tau) \tag{12}$$

$$C_{AC} = \frac{k_1 C_{G0}}{k_A.k_G}\left(\exp(-k_G\tau) - \exp(-k_A\tau)\right) \tag{13}$$

$$C_{Act} = \frac{k_2 C_{G0}}{k_5 - k_G}\left(\exp(-k_G\tau) - \exp(-k_5\tau)\right) \tag{14}$$

$$C_{Ad} = \frac{k_3 k_1 C_{G0}}{k_A - k_G}\left(\frac{k_A(1 - \exp(-k_G\tau)) - k_G(1 - \exp(-k_A\tau))}{k_A.k_G}\right) \tag{15}$$

$$C_{Mp} = \frac{k_4 k_1 C_{G0}}{k_A - k_G}\left(\frac{k_A(1 - \exp(-k_G\tau)) - k_G(1 - \exp(-k_A\tau))}{k_A.k_G}\right) \tag{16}$$

$$C_A = \frac{k_5 k_2 C_{G0}}{k_5 - k_G}\left(\frac{k_5(1 - \exp(-k_G\tau)) - k_G(1 - \exp(-k_5\tau))}{k_G.k_5}\right) \tag{17}$$

The concentrations of glycerol, acrolein, acetol, acetaldehyde, minor by-products, acetone, and initial concentration of glycerol are represented as C_{Gl}, C_{AC}, C_{Act}, C_{Ad}, C_{Mp}, C_A, and C_{G0}, respectively. Meanwhile, k_1 – k_5, k_G, and k_A are the reaction rate constants of R1 – R5, glycerol dehydration to acrolein and acetol, and acrolein decomposition, respectively.

The calculations of reaction rate constants are divided into three steps. Initially, the glycerol dehydration to acrolein and acetol rate constant (k_G) is determined from the conversion equation, Eq(18):

$$X_{Gl} = 1 - \exp(-(k_1 + k_2)\tau) \quad = 1 - \exp(-k_G.\tau) \tag{18}$$

Next, k_1 – k_5 and k_A are obtained by solving Eq(12)-(17) by the non-linear least square regression method in Polymath 6.10 software. Finally, all the differential equations were used to fit the experimental data.

Figure 2 exhibits the experimental data and calculated curves of glycerol conversion and different product yields versus W/F at 280, 300, 320, and 340 °C. The experimental data are explained well by the proposed reaction routes. Figure 2a-d clearly illustrate that increasing temperature from 280 to 340 °C significantly surged the pace of conversion increment to reach the maximum level (99%) at lower W/F. Also, the amount of acrolein production is reduced with the reaction temperature, particularly at higher W/F ratios of 2-3 ×10^3 kg-cat.s/m^3. Moreover, the production rate of by-products such as acetone, acetaldehyde, and minor products enhanced significantly at higher temperatures. Acetol production reached the peak at 320 °C reaction temperature and W/F ratios of 0.5–1 ×10^3 kg-cat.s/m^3 and then reduced at higher temperatures and W/F ratios (340 °C and W/F= 3 ×10^3 kg-cat.s/m^3). However, acetone and minor products yields increased steadily by rising the reaction temperature. Park et al. (2015) reported higher temperature reduces acrolein selectivity and enhances by-products yields. Reaction rate constants (k_1 – k_5, k_G, and k_A) derived from curve-fitting are summarized in Table 2. The last step in kinetic study is determination of activation energy (Ea) and frequency factor (A). Based on the Arrhenius equation, Eq(19), ln(k) versus inverse of temperature (1/T) is plotted in Figure 3. The activation energies (calculated from the slope) and the frequency factors (calculated from the intercept) are reported in Table 2.

$$\ln k = \ln A - \frac{E_a}{RT} \tag{19}$$

Table 2. Apparent kinetic parameters for the dehydration of glycerol over SiW$_{20}$-Al/Zr$_{10}$ catalyst calculated by the best fitted curve

rate constants $\left(\frac{m^3}{kg-cat.s}\right)$	Temperature (°C)				Ea (kJ/mol)	A $\left(\frac{m^3}{kg-cats}\right)$
	280	300	320	340		
k$_G$	1.05×10^{-3}	1.44×10^{-3}	2.12×10^{-3}	2.80×10^{-3}	46.9	27.7
k$_1$	9.24×10^{-4}	1.31×10^{-3}	1.86×10^{-3}	2.44×10^{-3}	46.0	20.7
k$_2$	1.27×10^{-4}	1.32×10^{-4}	2.61×10^{-4}	3.60×10^{-4}	53.3	12.1
k$_A$	6.87×10^{-5}	7.67×10^{-5}	7.72×10^{-5}	7.83×10^{-5}	5.7	2.5×10^{-4}
k$_3$	2.09×10^{-5}	2.30×10^{-5}	2.31×10^{-5}	2.35×10^{-5}	5.0	6.3×10^{-5}
k$_4$	4.78×10^{-5}	5.37×10^{-5}	5.41×10^{-5}	5.48×10^{-5}	6.1	1.8×10^{-4}
k$_5$	1.04×10^{-4}	1.43×10^{-4}	1.86×10^{-4}	2.89×10^{-4}	46.6	2.6
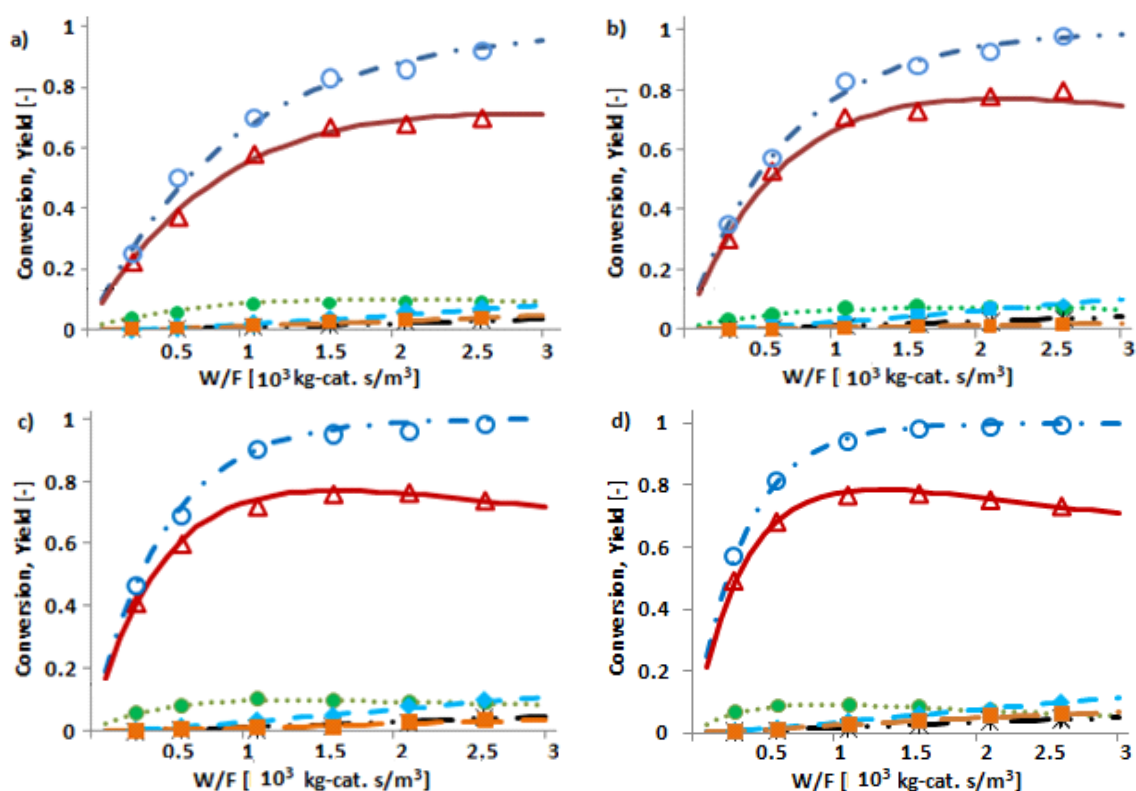
Figure 2. Glycerol conversions and product yields at (a) 280 °C, (b) 300 °C, (c) 320 °C, and (d) 340 °C, Experimental results: (○) Glycerol conversion, product yield (△) AC, (●) Act, (✳) Ad, (■) A, and (◆) Mp. Fitting results: (─ · ─) Glycerol conversion, product yield (────) AC, (·········) Act, (── · ·) Acd, (── ──) A, and (─ ─ ─) Mp.

The results in Table 2 and Figure 3 reveal that by increasing the reaction temperature from 280 to 340 °C, the rate constant for each reaction increased significantly. The rate constant of glycerol degradation to acrolein (k$_1$) is larger than glycerol to acetol (k$_2$) at the any of the investigated temperatures (Figure 3). Thus, a higher acrolein yield is obtained compared to the acetol.

The reaction rate constants for acetaldehyde (k$_3$) and minor products (k$_4$) or acrolein decomposition (k$_A$) are significantly smaller than the reaction rate constant of acrolein formation from glycerol (k$_1$) at the tested reaction temperatures (280 – 340 °C) as evident in Figure 3. The same trend is also reported previously (Akizuki et al., 2012). This indicates that just a little amount of acrolein is transformed to acetaldehyde and other minor products. Indeed, acrolein is a less reactive product and the hydrogenation of acrolein form minor products (e.g. propanal and allyl alcohol). In addition, the reaction rate constant of minor products (k$_4$) is higher than acetaldehyde (k$_3$). The activation energies reveal that acrolein formation required less activation energy (46.0 kJ/mol) compared to glycerol decomposition to acetol with 53.3 kJ/mol. It is obvious acetol

formation required the highest activation energy among the various products. Thus, high temperature increases acetol formation (Ramli et al., 2016). The 46.0 kJ/mol activation energy obtained in this study is far lower compared with 146 kJ/mol, which reported at supercritical water (SCW) condition for glycerol dehydration to acrolein (Watanabe et al., 2007).
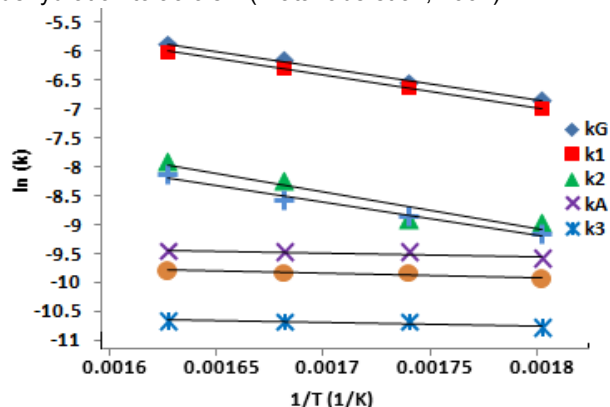

Figure 3. Arrhenius plot of the reaction rate constants for the estimation of activation energies (Ea) and frequency factors (A)

4. Conclusion

The kinetic study of gas-phase glycerol dehydration reaction in a packed-bed reactor using a supported solid acid catalyst (SiW$_{20}$-Al/Zr$_{10}$) was investigated. A kinetic model was established, based on the reaction mechanism. Consequently, all the related reaction rate constants and activation energies were determined. The findings of the kinetic study revealed all the rate constants increased with temperature, and the activation energies of glycerol dehydration to acrolein and acetol were 46.0 and 53.3 kJ/mol. The outcome of this study is suitable for further investigation on process modelling of a glycerol bio-refinery.

Reference

Akizuki M., Oshima Y., 2012, Kinetics of Glycerol Dehydration with WO$_3$/TiO$_2$ in Supercritical Water, Ind Eng Chem Res 51, 12253–12257.

Alhanash A., Kozhevnikova E.F., Kozhevnikov I.V., 2010, Gas-phase dehydration of glycerol to acrolein catalysed by caesium heteropoly salt, Appl Catal A: Gen 378, 11-18.

Atia H., Armbruster U., Martin A., 2008, Dehydration of glycerol in gas phase using heteropolyacid catalysts as active compounds, J Catal 258, 71-82.

Galy N., Nguyen R., Yalgin H., Thiebault N., Luart D., Len C., 2016, Glycerol in Sub- and Supercritical Solvents, J Chem Technol Biotechnol, DOI: 10.1002/jctb.5101.

Liu R., Lyu S., Wang T., 2016, Sustainable production of acrolein from biodiesel-derived crude glycerol over H$_3$PW$_{12}$O$_{40}$ supported on Cs-modified SBA-15, J Ind Eng Chem, 37,354-360.

Park H., Yun S., Kim T.Y., Lee K.R., Baek J., Yi J., 2015, Kinetics of the dehydration of glycerol over acid catalysts with an investigation of deactivation mechanism by coke, Appl Catal B: Environ 176,1-10.

Qadariyah L., Mahfud, Sumarno., Machudah S., Wahyudiono S., Sasaki M., Goto M., 2011, Degradation of glycerol using hydrothermal process, Bioresour Technol 102 (19), 9267-9271.

Ramli N.A.S., Amin N.A.S, 2016, Kinetic study of glucose conversion to levulinic acid over Fe/HY zeolite Catalyst, Chem Eng J 283, 150-159.

Talebian-Kiakalaieh A., Amin N.A.S., 2015, Kinetic Modeling, Kinetic Modeling, Thermodynamic, and Mass-Transfer Studies of Gas-Phase Glycerol Dehydration to Acrolein over Supported Silicotungstic Acid Catalyst, Ind Eng Chem Res 54, 8113.

Tsukuda E., Sato S., Takahashi R., Sodesawa T., 2007, Production of acrolein from glycerol over silica supported heteropoly acids, Catal Commun 8 (9), 1349-1353.

Watanabe M., Iida T.,Aizawa Y., Aida T.M., Inomata H., 2007, Acrolein synthesis from glycerol in hot-compressed water, Bioresour. Technol 98 (6), 1285-1290.